symmetry

MDPI

Article

Design, Synthesis and Cytotoxicity Screening of New Thiazole Derivatives as Potential Anticancer Agents through VEGFR-2 Inhibition

Tarfah Al-Warhi [1], Matokah Abualnaja [2], Ola A. Abu Ali [3], Najiah M. Alyamani [4], Fahmy G. Elsaid [5,6], Ali A. Shati [5], Sarah Albogami [7], Eman Fayad [7], Ali H. Abu Almaaty [8], Khaled O. Mohamed [9], Wael M. Alamoudi [10] and Islam Zaki [11,*]

1 Department of Chemistry, College of Science, Princess Nourah bint Abdulrahman University, P.O. Box 84428, Riyadh 11671, Saudi Arabia
2 Department of Chemistry, Faculty of Applied Science, Umm Al-Qura University, Makkah Al Mukarrama 24381, Saudi Arabia
3 Department of Chemistry, College of Science, Taif University, P.O. Box 11099, Taif 21944, Saudi Arabia
4 Biology Department, College of Science, University of Jeddah, Jeddah 23218, Saudi Arabia
5 Biology Department, Science, College, King Khalid University, Abha 61421, Saudi Arabia
6 Zoology Department, Faculty of Science, Mansoura University, Mansoura 35516, Egypt
7 Department of Biotechnology, Faculty of Sciences, Taif University, P.O. Box 11099, Taif 21944, Saudi Arabia
8 Zoology Department, Faculty of Science, Port Said University, Port Said 42526, Egypt
9 Pharmaceutical Organic Chemistry Department, Faculty of Pharmacy, Cairo University, Cairo 11562, Egypt
10 Department of Biology, Faculty of Applied Science, Umm Al-Qura University, Makkah Al Mukarrama 24382, Saudi Arabia
11 Pharmaceutical Organic Chemistry Department, Faculty of Pharmacy, Port Said University, Port Said 42526, Egypt
* Correspondence: eslam.zaki@pharm.psu.edu.eg

check for updates

Citation: Al-Warhi, T.; Abualnaja, M.; Abu Ali, O.A.; Alyamani, N.M.; Elsaid, F.G.; Shati, A.A.; Albogami, S.; Fayad, E.; Abu Almaaty, A.H.; Mohamed, K.O.; et al. Design, Synthesis and Cytotoxicity Screening of New Thiazole Derivatives as Potential Anticancer Agents through VEGFR-2 Inhibition. *Symmetry* **2022**, *14*, 1814. https://doi.org/10.3390/sym14091814

Academic Editor: György Keglevich

Received: 5 August 2022
Accepted: 26 August 2022
Published: 1 September 2022

Abstract: *Z*-configurated isomers are kinetically preferred molecules. Compounds with *Z*-configuration are contained in many natural products, biologically active compounds and as synthons for organic synthesis. Two series of new thiazole-based analogs were synthesized from appropriate starting materials hydrazinecarbothioamide derivatives (*Z*)**-2a,b** to be evaluated for their inhibitory activity towards VEGFR-2. The prepared thiazole compounds **3a-5b** were screened for their cytotoxic potency against the MDA-MB-231 breast cancer cell line and their percentage inhibition against VEGFR-2. Compound **4d** exhibited good VEGFR-2 inhibitory activity. A DNA flow cytometry analysis was conducted, and compound **4d** demonstrated cell cycle arrest at the G1 and G2/M phases of the cell cycle profile and an apoptosis-inducing effect by increasing the percentage of pre-G1 phase. Compound **4d** was further evaluated for its apoptosis-inducing effect by studying the effect on mitochondrial membrane potential (MMP) and p53 activation. It was found to boost the level of p53 and reduce the level of MMP compared with the untreated control cells.

Keywords: *Z*-configurated isomers; thiazole; hydrazinecarbothioamide; phenacylbromide; cytotoxicity; VEGFR-2; apoptosis; p53; mitochondrial membrane potential (MMP)

1. Introduction

Cancer is a major health problem with a complex pathogenesis, which threatens human life greatly [1,2]. Breast cancer is the second leading cause of cancer death for women [3]. A number of chemotherapeutic therapies have been developed to treat breast cancer, which include antiangiogenic agents and antimitotic agents [4,5]. Many natural compounds are known for their effective cancer treatment [6]. However, the complex chemical structure, difficult synthesis and formulation, in addition to the loss of oral availability, make these agents not suitable for the clinical treatment of breast cancer [7].

Therefore, there is considerable interest in the design and development of novel molecules that inhibit angiogenesis [8].

Tyrosine kinases are responsible for the transfer of phosphate group from ATP to the tyrosine residues in specific proteins inside a cell [9]. This phosphorylation leads to a change in many cellular functions [10]. They are considered as important mediators involved in signaling pathways [11]. Mutation can cause some tyrosine kinases to become continuously active, leading to the development of malignancy [12]. Vascular endothelial growth factor receptor-2 (VEGFR-2) is a receptor of tyrosine kinase and is one of the major regulators of physiological and pathological vascular endothelial cells growth [13]. VEGFR-2 is overexpressed in tumor vascular cells which promote vascular proliferation [14]. Some VEGFR-2-targeted inhibitor agents have been developed and used in experimental studies to monitor tumor angiogenesis and treatment efficacy [15]. The main structural characteristics of VEGFR-2 inhibitors consist of two main head and tail parts [16]. The head part is formed from a heterocyclic ring of five-, six- or even seven-membered heterorings such as furan, pyrazole, pyridine or benzodiazepine rings that bind the hydrophobic ATP-binding domain, and the tail part is bound to the allosteric site of the enzyme [17,18]. The tail part is sectioned into two main parts: a hydrophilic linker and a hydrophobic tail [19]. The hydrophilic linker group has an H-bond acceptor–donor pair (HBA/HBD) domain which can be urea, thiourea or carbohydrazide [20]. The hydrophobic tail consists of aryl groups capable of forming hydrophobic interactions [21]. Sorafenib **I** is a multitarget receptor tyrosine kinase inhibitor of several receptors mainly VEGFR-2 [22]. It represents a typical pharmacophoric feature of VEGFR-2 inhibitors where a central aryl ring attached to a pyridine ring via an ether linker as the head part and is also attached to the terminal aryl ring via a urea moiety [23].

Thiazoles are considered to be important chemical synthons found in a variety of pharmacologically active compounds [24]. They possess a wide range of biological activities as anticancer, antimicrobial and anti-inflammatory agents [25–27]. Hydrazinyl thaizole molecule **II** displayed potent antitumor activity against the C6 cell line with an IC_{50} value of 3.83 μM compared with that of cisplatin as a reference drug (IC_{50} = 12.67 μM) [28]. In addition, compound **III** possessing a 4-chlorophenylthiazole ring was found to inhibit the kinase activity of VEGFR-2 with an IC_{50} value of 51.09 nM compared with sorafenib's IC_{50} of 51.41 nM [29]. Moreover, hydrazinyl thiazole derivative **IV** exhibited a promising cytotoxic activity via good EGFR-TK inhibition [30] (Figure 1).

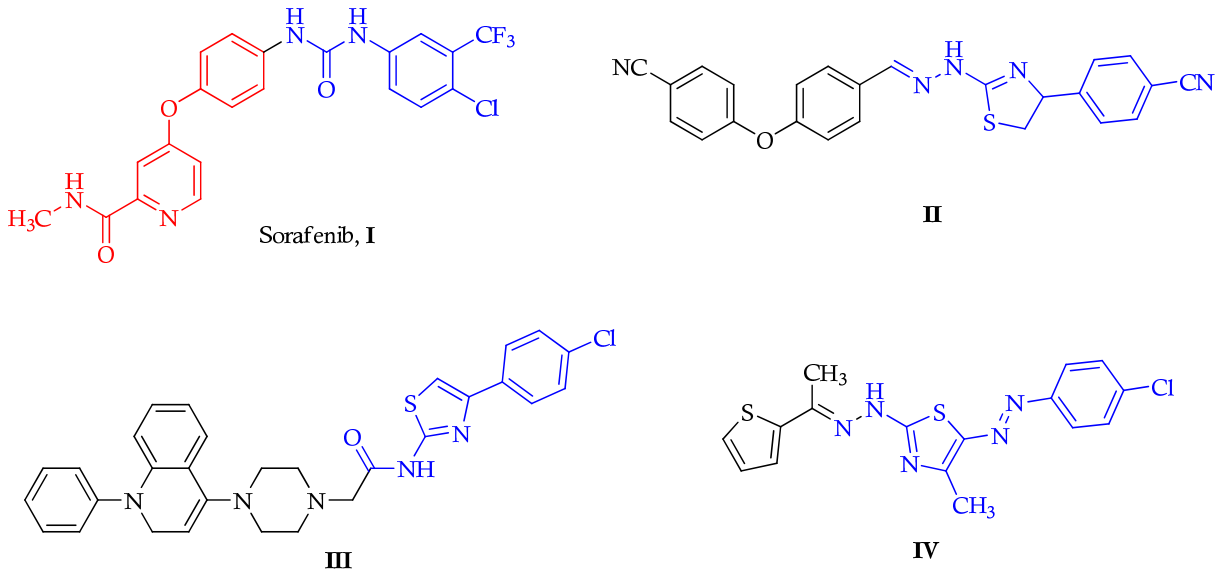

Figure 1. Chemical structure of sorafenib (**I**) and some bioactive thiazole derivatives (**II**–**IV**).

In an attempt to discover potential VEGFR-2 inhibitors, a new series of thiazole-based derivatives **3a-5b** was designed and synthesized as VEGFR-2 tyrosine kinase inhibitors (Figure 2). The prepared thiazole compounds were evaluated for their cytotoxic activity in vitro against the MDA-MB-231 breast cancer cell line. In order to investigate the mechanistic pathways of antiproliferative activity of the constructed thiazole compounds, the most potent cytotoxic compounds were chosen to perform extra investigations such as the VEGFR-2 inhibitory activity, cell cycle analysis and apoptosis related assays.

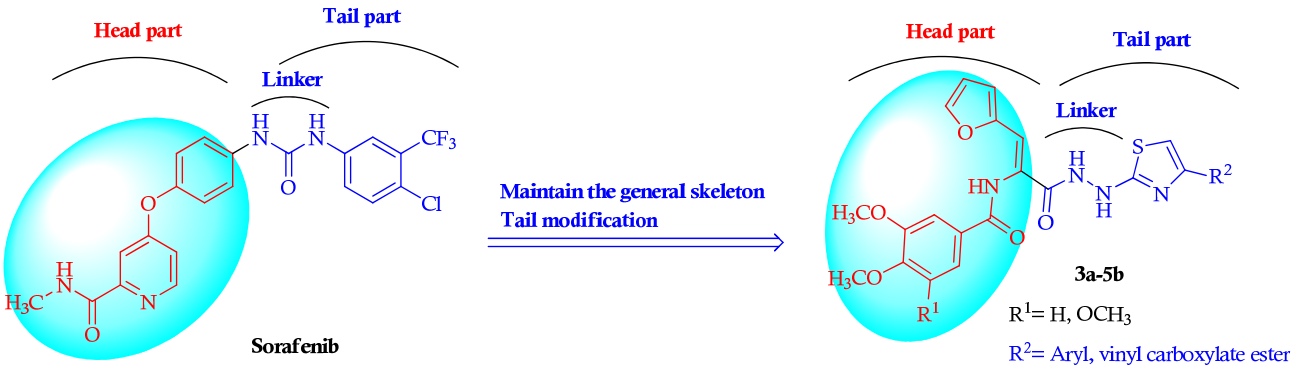

Figure 2. Design strategy of the prepared thiazole-based compounds **3a-5b**.

2. Results and Discussion

2.1. Chemistry

In Scheme 1, we report the synthetic route utilized to obtain the target thiazolyl derivatives **3a-5b**. The treatment of oxazolones (*Z*)**-1a,b** with thiosemicarbazide in absolute ethanol under reflux gave the *Z*-configurated isomer hydrazine carbothioamides (*Z*)**-2a,b.** The hydrazine carbothioamides (*Z*)**-2a,b** were utilized as synthons for the synthesis of thiazole derivatives **3a-5b.** The ^{1}H-NMR spectrum of hydrazinecarbothioamide derivative (*Z*)**-2a**, for example, revealed the presence of five signals at δ 8.04, 8.64, 9.43, 10.03 and 10.32 ppm assigned to NH and NH_2 protons. In addition, the ^{13}C-NMR spectrum of compound (*Z*)**-2a** exhibited three signals at δ 164.17, 16.78 and 181.65 ppm attributed to two carbonyl (C=O) and thioamide (C=S) groups, respectively.

The thioamide group in the aforementioned hydrazinecarbothioamide derivatives (*Z*)**-2a,b** was subjected to a cyclization reaction through the reaction of the appropriate hydrazinecarbothioamide derivative (*Z*)**-2a,b** with a respective (un)substituted phenacyl bromide in pure ethanol and sodium acetate anhydrous (NaOAc) to yield the corresponding arylthiazolyl derivatives **3a-4e**. The chemical structures of the prepared arylthiazolyl derivatives **3a-4e** were elucidated on the basis of the ^{1}H-NMR and ^{13}C-NMR spectral data. The ^{1}H-NMR spectra of 3-nitrophenylthiazolyl derivative **4d**, as a representative example, displayed the appearance of a characteristic signal at δ 7.59 ppm corresponding t the H-4 thiazole ring as well as the presence of characteristic signals at δ 9.73, 9.90 and 10.62 ppm corresponding to three NH protons. In addition, the ^{1}H-NMR spectrum of 3-nitrophenylthiazolyl derivative **4d** showed the appearance of new proton peaks in the aromatic region corresponding to the phenyl protons of the 3-nitrophenylthiazolyl moiety. Moreover, the ^{13}C-NMR spectrum of 3-nitrophenylthiazolyl derivative **4d** showed the appearance of signal at δ 173.51 ppm due to the C2 thiazole carbon in addition to the presence of the characteristic signals of aromatic carbons related to phenyl carbons of the 3-nitrophenylthiazolyl moiety.

In addition, the thiazolyl ester derivatives **5a,b** were synthesized by the reaction of appropriate hydrazinecarbothioamide (*Z*)**-2a,b** with ethyl 4-chloroacetoacetate in dry DMF and potassium carbonate anhydrous (K_2CO_3). The structure of the novel thiazolyl ester derivatives **5a,b** was established using ^{1}H-NMR and ^{13}C-NMR spectral data. The ^{1}H-NMR spectrum of **5b**, for example, displayed a triplet signal at δ 1.19 ppm attributed to methyl (CH_3) ester and a quartet signal at δ 3.75 ppm for the methylene (CH_2) ester, in addition

to a singlet signal at δ 3.54 ppm representing the methylene (CH_2) group of the thiazole ring. Moreover, the ^{1}H-NMR spectrum of compound **5b** showed three characteristic NH signals at δ 9.41, 9.86 and 10.48 ppm. The ^{13}C-NMR spectrum of compound **5b** highlighted new upfield signals at δ 14.57 and 60.69 ppm for the OCH_2CH_3 ester carbons as well as a signal at δ 37.52 ppm attributed to the methylene (CH_2) carbon of the thiazole ring. Furthermore, the ^{13}C-NMR spectrum of compound **5b** showed a signal at δ 173.03 ppm due to the carbonyl (C=O) ester carbon.

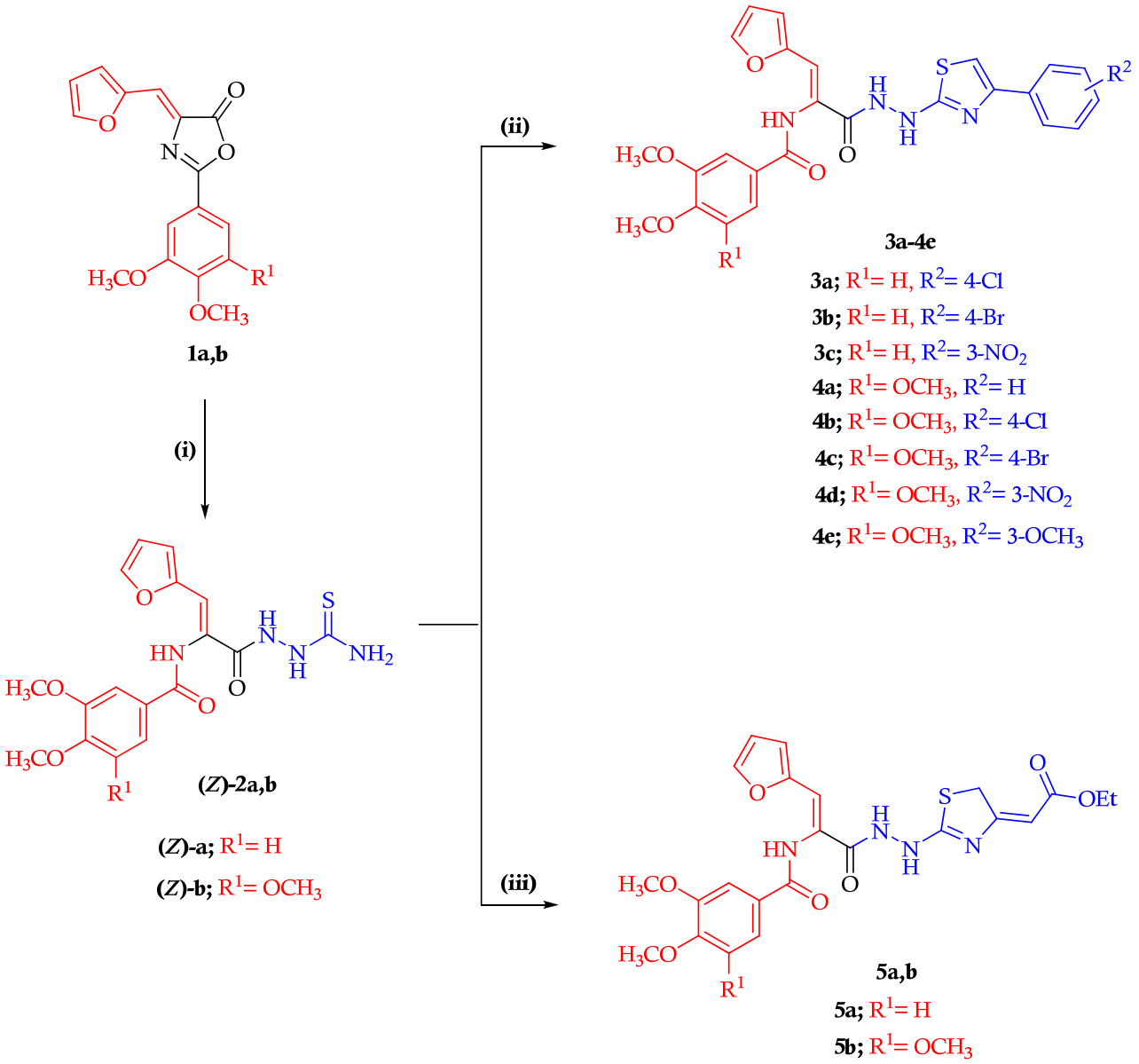

Scheme 1. Synthesis of the target compounds **3a-5b**. Reagents and reaction condition: (**i**) thiosemicarbazide, EtOH; (**ii**) respective (un)substituted phenacyl bromide, NaOAc and EtOH; (**iii**) ethyl 4-chloroacetoacetate, K_2CO_3 and DMF.

2.2. Biology

2.2.1. Cytotoxic Activity against MDA-MB-231 Breast Cancer Cell Line

All the newly synthesized aryl thiazole molecules **3a-4e** and ester thiazole derivatives **5a,b** were evaluated for their in vitro cytotoxic activity against the MDA-MB-231 breast cell line utilizing an MTT antiproliferative assay using sorafenib as the reference drug. The results were recorded as half-maximal inhibitory concentration (IC_{50}) values. The

results presented in Table 1 reveal that in general all the tested compounds possessed a moderate to good cytotoxic activity against the MDA-MB-231 cell line. On the basis of the obtained IC_{50} values against MDA-MB-231 cells, compounds 4-chlorophenylthiazolyl **4b**, 4-bromophenylthiazolyl **4c** and 3-nitrophenylthiazolyl **4d** were found to be the most effective cytotoxic compounds against MDA-MB-231 cells with IC_{50} values of 3.52, 4.89 and 1.21 μM, respectively, in comparison to sorafenib (IC_{50} = 1.18 μM) (Table 1). Besides **4b**, **4c** and **4d**, compounds **3a-3c** and **4e** showed a moderate cytotoxic activity against MDA-MB-231 cells. According to the current study, a comparative analysis between the synthesized compounds revealed that in general compounds containing a halogen or nitro substituent showed better cytotoxic activity than the unsubstituted phenyl **4a** or 3-methoxy-substituted **4e** derivatives. In addition, regarding the corresponding 3-nitrophenyl group, the results revealed that the replacement of the nitro group with another group resulted in a decrease of the cytotoxic activity.

Table 1. Cytotoxic screening of the tested thiazole derivatives **3a-5b**. Data expressed as the mean ± SD.

Comp No.	IC_{50} Value (μM)
	MDA-MB-231
3a	8.12 ± 0.42
3b	9.55 ± 0.46
3c	7.39 ± 0.41
4a	29.77 ± 3.27
4b	3.52 ± 0.18
4c	4.89 ± 0.24
4d	1.21 ± 0.09
4e	13.33 ± 0.93
5a	24.89 ± 1.19
5b	19.25 ± 0.68
Sorafenib	1.18 ± 0.06

2.2.2. Vascular Endothelium Growth Factor-2 (VEGFR-2) Inhibitory Activity

To cast light onto the mechanism of action of the prepared thiazole derivatives, the VEGFR-2 inhibitory activity of our designed compounds 4-chlorophenylthiazolyl **4b**, 3-nitrophenylthiazolyl **4d** and 3-methoxyphenylthiazolyl **4e** was studied using an ELISA analysis. Sorafenib was utilized as a reference standard in the current study. The results in Figure 3 demonstrate that 4-chlorophenylthiazole **4b** and 3-nitrophenylthiazole **4d** showed a good inhibitory activity against VEGFR-2 which caused an 81.36 and 85.72% inhibition percentage compared with sorafenib (86.93%). These data pointed out that the presence of an electron-withdrawing group at the phenyl group of the arylthiazolyl moiety might be the reason for a better VEGFR-2 enzyme inhibitory activity. On the other hand, the VEGFR-2 percentage inhibition showed by 3-methoxyphenylthiazolyl derivative **4e** was recorded as 38.22% in comparison with sorafenib. In conclusion, the results correlated the good cytotoxic activity of compounds **4b** and **4d** to their abilities to inhibit VEGFR-2 enzyme.

2.2.3. Cell Cycle Analysis of Compound **4d**

To confirm the mechanism of action of these thiazole derivatives, a cell cycle analysis was performed. For this experiment, MDA-MB-231 cells were treated with compound **4d** for 48 h at a concentration equal to its IC_{50} concentration (IC_{50} = 1.21 μM). The results showed that 3-nitrophenylthiazole molecule **4d** displayed both G1 and G2/M phases accumulation, which strongly suggested that its cytotoxic activity was due to the effect on VEGFR-2 in MDA-MB-231 cells. Furthermore, the results demonstrated that 3-nitrophenylthiazolyl molecule **4d** increased the accumulation of cells at both G1 and G2/M phases by 1.2- and 2.2-fold, respectively, compared to untreated controls, which indicated a cell cycle blockade at the G1 and G2 phases. Finally, the results suggested that the test 3-nitrophenylthiazole

molecule **4d** resulted in a cell cycle blockade at the G1 and G2/M phases in the treated MDA-MB-231 cells (Figure 4).

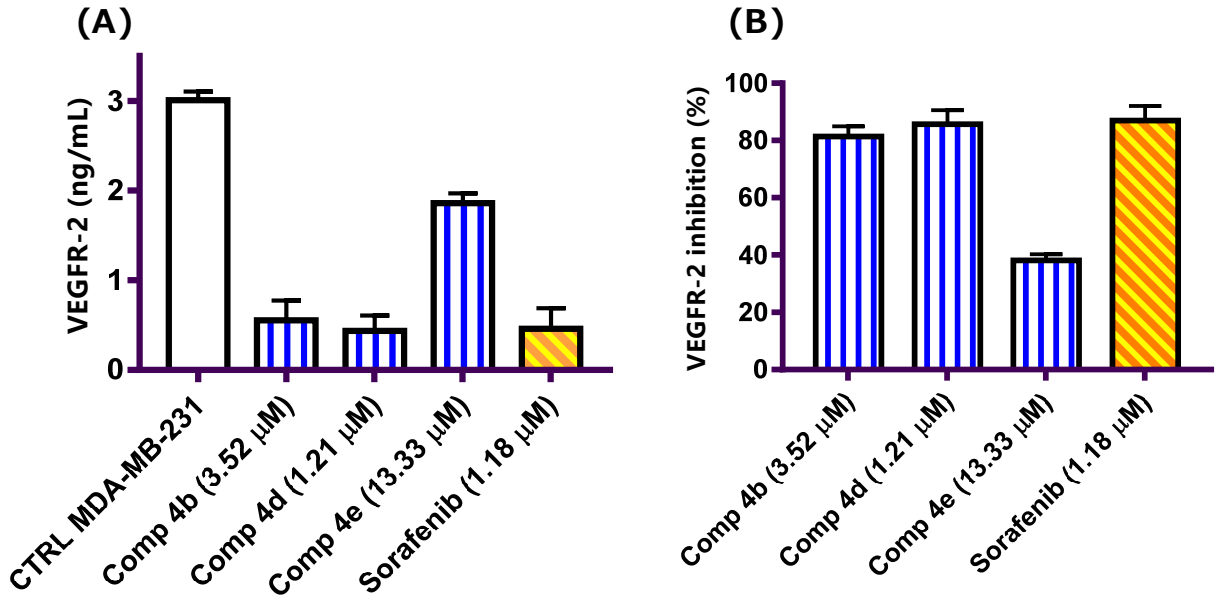

Figure 3. Compounds **4b**, **4d** and **4e** inhibited VEGFR-2 in MDA-MB-231 cells. (**A**) MDA-MB-231 cells were treated with 3.52, 1.21, 13.33 and 1.18 µM of compounds **4b**, **4d** and **4e** and sorafenib, respectively, and VEGFR-2 concentration was determined by ELISA analysis. (**B**) VEGFR-2 inhibition percentage induced by compounds **4b**, **4d** and **4e** compared to sorafenib at their IC_{50} concentration (µM).

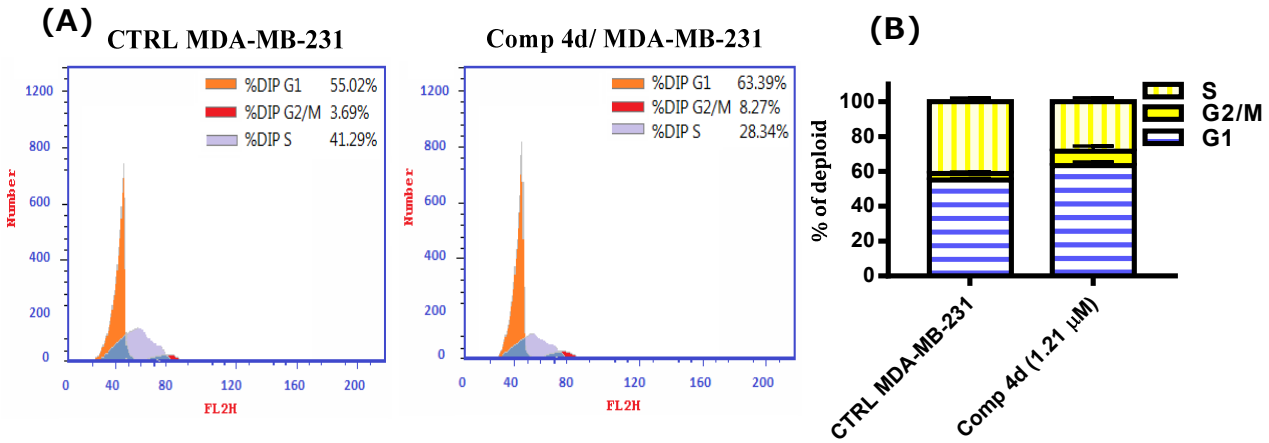

Figure 4. Compound **4d** induced both G1 and G2/M phase arrest in MDA-MB-231 cells. (**A**) MDA-MB-231 cells were treated with 1.21 µM of compound **4d** for 48 h. Cell cycle analysis was quantized by PI and FACS analysis using image-based cytometry. (**B**) The percentage of cells in different phases was quantified.

2.2.4. Annexin V/FITC Apoptosis Staining Assay

In order to study whether cell death induced by 3-nitrophenylthiazolyl derivative **4d** treatment was related to apoptosis or necrosis, the Annexin V-FITC/PI staining assay was carried out using a FACS analysis. MDA-MB-231 cells were treated with compound **4d** at a concentration equal to its IC_{50} concentration (IC_{50} = 1.21 µM) for 48 h. Thiazole derivative **4d** caused a marked accumulation of annexin V positive cells and induced both early and late apoptosis compared to untreated control cells. Results presented in Figure 5 revealed that subjecting MDA-MB-231 cells to compound **4d** led to 57.1-fold increase in early apoptosis and a 51.4-fold increase in the percentage of late apoptotic cells compared

with the negative control cells. On the other hand, the percentage of necrotic cells was increased by fivefold compared to the negative control. Based on the findings of the cell cycle arrest and apoptosis assays, it appears that 3-nitrophenylthiazolyl molecule **4d** could induce cellular apoptosis in MDA-MB-231 cells.

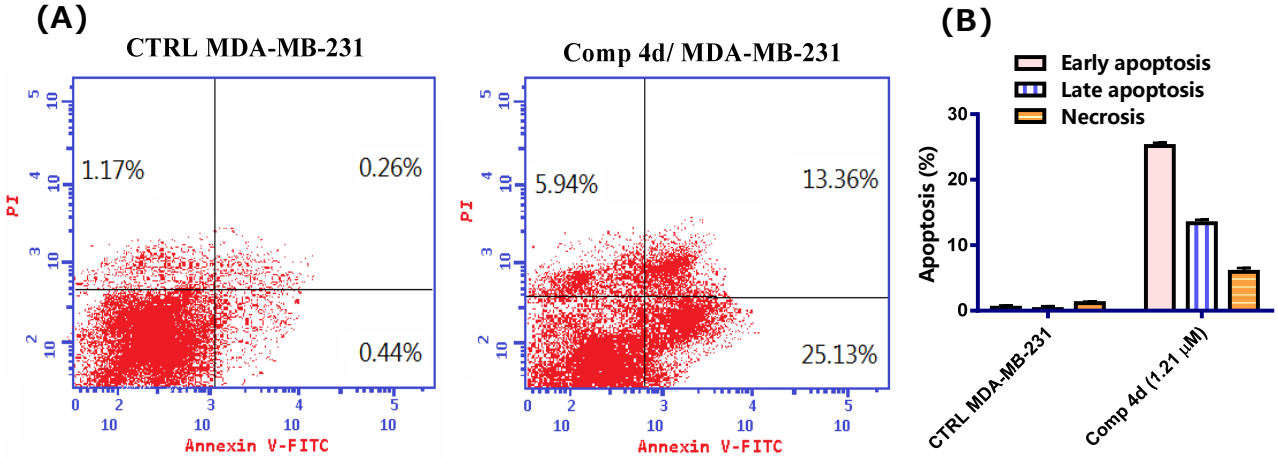

Figure 5. Compound **4d** induced apoptosis in MDA-MB-231 cells. (**A**) MDA-MB-231 cells were treated with 1.21 μM of compound **4d** for 48 h. Cell apoptosis was quantized by an Annexin V-FITC/PI dual staining assay using image-based cytometry. (**B**) The quantification of MDA-MB-231 cellular apoptosis.

2.2.5. Mitochondrial Membrane Potential (MMP)

Apoptosis is an important potential target for therapeutic intervention [31]. Most cells are programmed to stop proliferation or kill themselves via the mitochondrial apoptotic pathway if survival signals are not regularly received from their environment due to the altering of the mitochondrial membrane potential (MMP) [32]. Studies have demonstrated that VEGFR-2 and tubulin inhibitors are capable of decreasing the level MMP resulting in a release of cytochrome c and other proapoptotic markers, which in turn leads to the activation of the intrinsic cellular apoptosis pathway [33]. To evaluate the effect of thiazole molecule **4d** on the level of MMP, MDA-MB-231 cells were treated with 3-nitrophenylthiazolyl derivative **4d** at its IC_{50} concentration (IC_{50} = 1.21 μM) for 48 h (Figure 6). The data showed that compound **4d** reduced the level of MMP by almost 3.70-fold compared with negative control cells, indicating that **4d** possessed the ability to induce intrinsic cellular apoptosis in MDA-MB-231 breast cancer cells.

2.2.6. In Vitro ELISA Measurement of the Level of p53

p53 is a transcription factor which regulates cell cycle growth and is very important in cancer because of its large number of downstream targets [34]. p53 can either inhibit cell cycle entry or induce apoptosis, thus it is a multifaceted tumor suppressor and plays a key role in the defense against cancer [35]. Moreover, p53 can decrease the synthesis of VEGF and inhibit tumor-cell-induced angiogenesis [36]. In order to study the mediated mechanistic pathway of apoptosis in treated cells with 3-nitrophenylthiazolyl derivative **4d**, the concentration of p53 was measured using an ELISA. The data demonstrated that there was an increased level of p53 induction after treatment with 3-nitrophenylthiazolyl molecule **4d** by 9.14-fold more than in the negative control group (Figure 7). According to the obtained data, the proapoptotic-inducing abilities of 3-nitrophenylthiazolyl molecule **4d** were caused by p53 activation, which boosted the induction of cellular apoptosis through the mitochondrial apoptotic pathway.

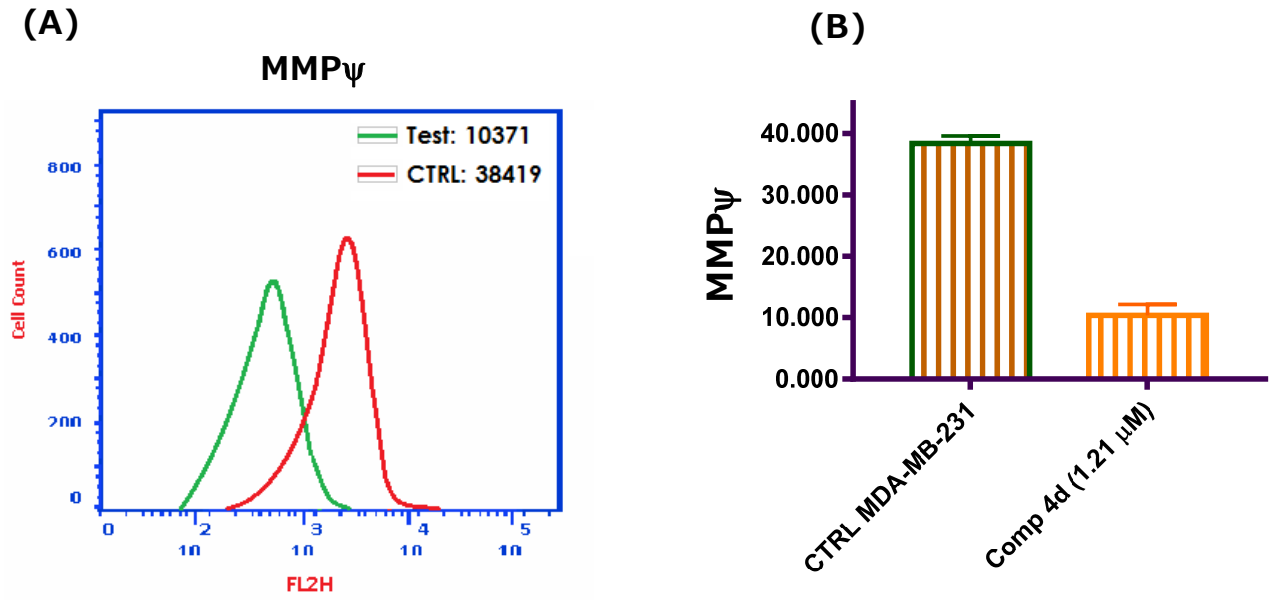

Figure 6. Compound **4d** promoted MMP depolarization in MDA-MB-231 cells. (**A**) MDA-MB-231 cells were treated with 1.21 μM of compound **4d** for 48 h. MMP was quantified using image-based flow cytometry. (**B**) The quantification of MMP in MDA-MB-231 cells after treatment with compound **4d** at its IC_{50} concentration (μM).

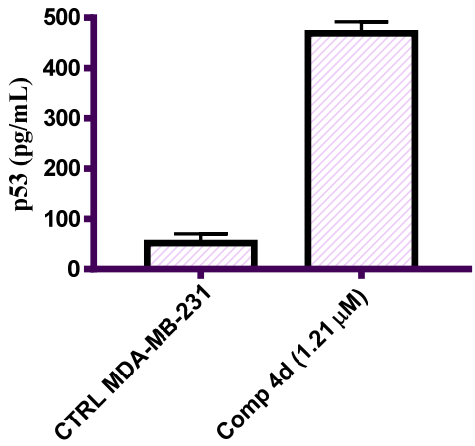

Figure 7. Graphical representation of the effect of 3-nitrophenylthiazolyl molecule **4d** on the level of p53 in MDA-MB-231 cells for 48 h.

2.2.7. Molecular Docking Study

Molecular docking simulation was performed with the VEGFR-2 crystal structure (PDB ID: 4ASD) by molecular operating environment MOE 2015.10. The molecular docking study was performed for 3-nitrophenylthiazolyl molecule **4d** into the active site of VEGFR-2 with the aim to gain more insight on the binding mode of this compound. Docking results revealed that the docking score achieved by 3-nitrophenylthiazolyl molecule **4d** was −12.18 kcal/mol. As can be seen in (Figure 8), the 3-nitrophenylthiazolyl **4d** interacted with the carbonyl group (C=O) of the hydrazine group as H-bond acceptor with the key amino acid Arg 1027. As a hydrogen bond donor, it interacted with the nitro group (NO_2) of the 3-nitrophenyl thiazolyl moiety with the key amino acid Cys 817. The phenyl group of the 3-nitrophenylthiazolyl moiety interacted as a hydrogen bond donor with Glu 818. Additionally, there was a hydrophobic interaction between the phenyl group of the 3-nitrophenylthiazolyl moiety with the hydrophobic side chains of the amino acid Glu 815. From the obtained results, molecular modeling studies of 3-nitrophenylthiazolyl derivative

4d revealed that the interaction result is in line with the obtained data against VEGFR-2 inhibition and justifies the observed chemicals findings.

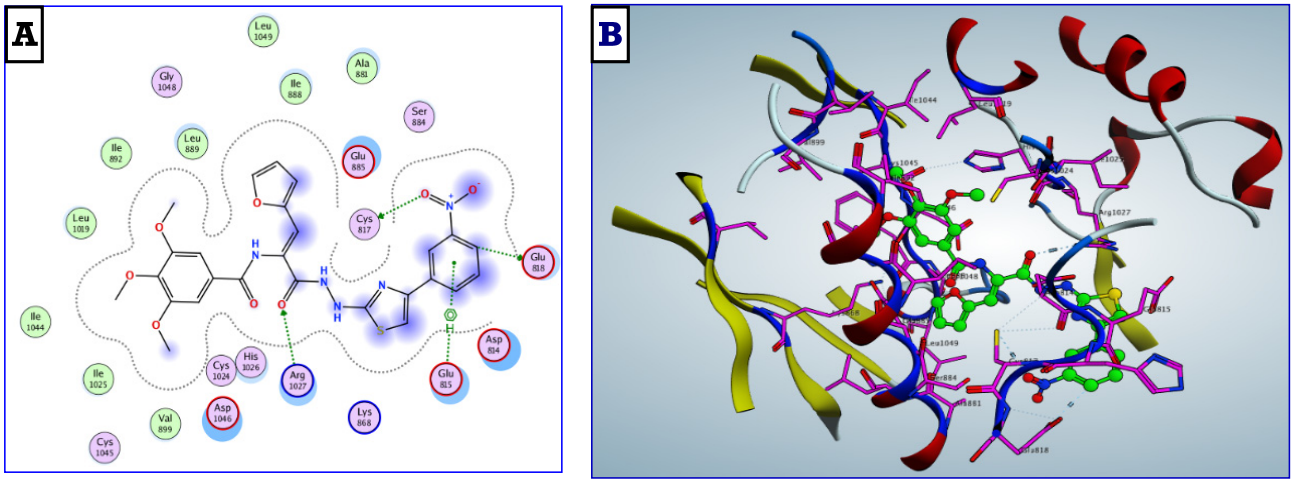

Figure 8. The binding poses (2D and 3D) of 3-nitrophenylthiazolyl molecule **4d** in VEGFR-2 active site (PDB ID: 4ASD). (**A**) 2D representation; (**B**) 3D representation.

3. Conclusions

In conclusion, two new series of synthetic thiazole-based molecules **3a-5b** were designed and synthesized as anti-VEGFR-2 agents. The chemical structure of the prepared thiazole derivatives **3a-5b** was elucidated on the basis of ^{1}H-NMR and ^{13}C-NMR spectra along with an elemental microanalysis. The prepared thiazole derivatives **3a-5b** were screened for their cytotoxic potency against the MDA-MB-231 breast cancer cell line and their percentage inhibition against VEGFR-2. The cytotoxicity screening demonstrated that 4-chlorophenylthiazolyl **4b** and 3-nitrophenylthiazolyl **4d** derivatives displayed the highest cytotoxic activity with IC_{50} values of 3.52 and 1.21 μM, respectively, compared with sorafenib (IC_{50} = 1.18 μM) as a reference compound. 4-Chlorophenylthiazolyl **4b** and 3-nitrophenylthiazolyl **4d** derivatives showed good VEGFR-2 enzyme inhibition which was 81.36 and 85.72% inhibition compared to sorafenib (86.93% enzyme inhibition). A DNA flow cytometry analysis for the 3-nitrophenylthiazolyl **4d** derivative demonstrated a cell cycle arrest at the G1 and G2/M phases by 1.23- and 2.20-fold, respectively, compared to the negative control group. Moreover, 3-nitrophenylthiazolyl **4d** molecule showed proapoptotic activity by inducing a marked increase in the percentage of the pre-G1 phase by almost 23.80-fold in an apoptosis-staining study compared with the negative control group. The apoptosis mechanistic pathway of 3-nitrophenylthiazolyl derivative **4d** indicated that it boosted the level of p53 by 9.14-fold as well as reduced the level of MMP by 3.70-fold compared with the control MDA-MB-231 cells.

4. Experimental Methods

4.1. Chemistry

4.1.1. General

Melting points were determined in open capillaries tube using Electrothermal Digital melting point apparatus and were uncorrected. ^{1}H-NMR and ^{13}C-NMR spectra were obtained with a Bruker 400 MHz DRX-Avance NMR spectrometer, peaks positions are given in ppm downfield from tetramethylsilane (TMS) as the internal standard. Elemental analyses were performed on Elementar, Vario El, Microanalytical unit, Cairo, Egypt and were found within ±0.4% of the theoretical values.

4.1.2. General Procedure for the Synthesis of (Z)-*N*-(3-(2-Carbamothioylhydrazinyl)-1-(furan-2-yl)-3-oxoprop-1-en-2-yl)arylamides (Z)-**2a,b**

A mixture of 2-aryl-4-(furan-2-ylmethylene)oxazol-5(4*H*)-one **1a,b** (10 mmol) and thiosemicarbazide (12 mmol) in 20 mL of pure ethanol was heated to reflux with stirring for 6–8 h. The reaction mixture was concentrated under reduced pressure to remove the excess ethanol. The obtained solid residue was filtered, washed with ethanol, dried and purified by crystallization using ethanol/H_2O (3:1) to obtain the title compound **2a,b**.

(Z)-*N*-(3-(2-Carbamothioylhydrazinyl)-1-(furan-2-yl)-3-oxoprop-1-en-2-yl)-3,4-dimethoxybenzamide ((Z)-**2a**)

Pale yellow powder (231 mg, 59%), m.p. 184–186 °C. ^{1}H-NMR (400 MHz, DMSO-d_6, δ ppm): 3.85 (s, 3H, OCH_3), 3.85 (s, 3H, OCH_3), 6.62 (s, 1H, furan CH), 6.78 (s, 1H, furan CH), 7.01 (s, 1H, arom.CH), 7.11 (d, *J* = 8.5 Hz, 1H, arom.CH), 7.20 (s, 1H, olefinic CH), 7.62 (s, 1H, arom.CH), 7.81 (s, 1H, furan CH), 8.04 (s, 1H, NH), 8.64 (s, 1H, NH), 9.43 (s, 1H, NH), 10.03 (s, 1H, NH), 10.32 (s, 1H, NH). ^{13}C-NMR (100 MHz, DMSO-d_6, δ ppm): 56.15 (OCH_3), 56.19 (OCH_3), 111.41 (C5 dimethoxybenzamide), 111.81 (C2 dimethoxybenzamide), 115.26 (C3 furan), 116.79 (C4 furan), 120.41 (C olefinic), 122.14 (C6 dimethoxybenzamide), 126.10 (C olefinic), 126.18 (C1 dimethoxybenzamide), 145.36 (C5 furan), 148.65 (C2 furan), 149.96 (C3 dimethoxybenzamide), 152.41 (C4 dimethoxybenzamide), 164.17 (C=O thiosemicarbazone), 166.78 (C=O dimethoxybenzamide), 181.65 (C=S). Anal. Calcd. for $C_{17}H_{18}N_4O_5S$ (390.41): C, 52.30; H, 4.65; N, 14.35. Found: C, 52.44; H, 4.73; N, 14.18.

(Z)-*N*-(3-(2-Carbamothioylhydrazinyl)-1-(furan-2-yl)-3-oxoprop-1-en-2-yl)-3,4,5-trimethoxybenzamide ((Z)-**2b**)

Orange powder (259 mg, 62%), m.p. 194–196 °C. ^{1}H-NMR (400 MHz, DMSO-d_6, δ ppm): 3.75 (s, 3H, OCH_3), 3.87 (s, 6H, 2OCH_3), 6.62 (dd, *J* = 3.4, 1.8 Hz, 1H, furan CH), 6.81 (d, *J* = 3.4 Hz, 1H, furan CH), 7.05 (s, 1H, arom.CH), 7.13 (s, 1H olefinic CH), 7.37 (s, 2H, arom.CH), 7.83 (d, *J* = 1.5 Hz, 1H, furan CH), 8.04 (s, 1H, NH), 8.64 (s, 1H, NH), 9.45 (s, 1H, NH), 10.12 (s, 1H, NH), 10.32 (s, 1H, NH). Anal. Calcd. for $C_{18}H_{20}N_4O_6S$ (420.44): C, 51.42; H, 4.79; N, 13.33. Found: C, 51.53; H, 4.71; N, 13.21.

4.1.3. General Procedure for the Synthesis of (Z)-*N*-(3-(2-(4-Arylthiazol-2-yl)hydrazinyl)-1-(furan-2-yl)-3-oxoprop-1-en-2-yl)arylamides **3a-4e**

A mixture of appropriate hydrazinecarbothioamide **2a,b** (10 mmol), appropriate (un)substituted phenacyl bromide (10 mmol) and sodium acetate anhydrous (984 mg, 12 mmol) in 20 mL pure ethanol was heated to reflux for 2–3 h. The reaction progress was followed up by a TLC analysis. After completion of the reaction, the obtained solid residue was filtered, washed with 10 mL ethanol, dried and crystallized from ethanol/H_2O (3:1) to give the title products **3a-4e**.

(Z)-*N*-(3-(2-(4-(4-Chlorophenyl)thiazol-2-yl)hydrazinyl)-1-(furan-2-yl)-3-oxoprop-1-en-2-yl)-3,4-dimethoxybenzamide (**3a**)

White powder (382 mg, 67%), m.p. 218–220 °C. ^{1}H-NMR (400 MHz, DMSO-d_6, δ ppm): 3.85 (s, 6H, 2OCH_3), 6.58–6.66 (m, 1H, furan CH), 6.78 (d, *J* = 3.4 Hz, 1H, furan CH), 7.10 (d, *J* = 8.4 Hz, 1H, arom.CH), 7.14 (s, 1H, olefinic CH), 7.32 (s, 1H, thiazole CH), 7.45 (d, *J* = 8.5 Hz, 2H, arom.CH), 7.65 (s, 1H, arom.CH), 7.70 (d, *J* = 8.5 Hz, 1H, furan CH), 7.81 (s, 1H, arom.CH), 7.86 (d, *J* = 8.4 Hz, 2H, arom.CH), 9.60 (s, 1H, NH), 9.79 (s, 1H, NH), 10.56 (s, 1H, NH). ^{13}C-NMR (100 MHz, DMSO-d_6, δ ppm): 56.10 (OCH_3), 56.14 (OCH_3), 104.39 (C5 thiazole), 111.37 (C5 dimethoxybenzamide), 111.80 (C2 dimethoxybenzamide), 112.86 (C3 furan), 114.80 (C4 furan), 118.22 (C olefinic), 121.93 (C6 dimethoxybenzamide), 126.43 (C olefinic), 126.95 (C1 dimethoxybenzamide), 127.72 (C2,6 chlorophenyl), 129.02 (C3,5 chlorophenyl), 132.27 (C1 chlorophenyl), 134.06 (C4 chlorophenyl), 145.21 (C5 furan), 148.66 (C2 furan), 149.70 (C4 thiazole), 149.97 (C3 dimethoxybenzamide), 152.16 (C4 dimethoxybenzamide), 165.37 (C=O hydrazide), 165.76 (C=O dimethoxybenzamide), 173.20

(C2 thiazole). Anal. Calcd. for $C_{25}H_{21}BrN_4O_5S$ (569.43): C, 52.73; H, 3.72; N, 9.84. Found: C, 52.66; H, 3.78; N, 9.98.

(Z)-*N*-(3-(2-(4-(4-Bromophenyl)thiazol-2-yl)hydrazinyl)-1-(furan-2-yl)-3-oxoprop-1-en-2-yl)-3,4-dimethoxybenzamide (**3b**)

White powder (374 mg, 71%), m.p. 215–217 °C. ^{1}H-NMR (400 MHz, DMSO-d_6, δ ppm): 3.85 (s, 6H, 2OCH_3), 6.61 (dd, *J* = 3.4, 1.8 Hz, 1H, furan CH), 6.78 (d, *J* = 3.4 Hz, 1H, furan CH), 7.10 (d, *J* = 8.5 Hz, 1H, arom.CH), 7.14 (s, 1H, olefinic CH), 7.33 (s, 1H, thiazole CH), 7.58 (d, *J* = 8.6 Hz, 2H, arom.CH), 7.65 (d, *J* = 1.9 Hz, 1H, arom.CH), 7.70 (dd, *J* = 8.4, 1.9 Hz, 1H, furan CH), 7.78 (s, 1H, arom.CH), 7.81 (d, *J* = 8.4 Hz, 2H, arom.CH), 9.60 (s, 1H, NH), 9.79 (s, 1H, NH), 10.56 (s, 1H, NH). ^{13}C-NMR (100 MHz, DMSO-d_6, δ ppm): 56.10 (OCH_3), 56.14 (OCH_3), 104.49 (C5 thiazole), 111.37 (C5 dimethoxybenzamide), 111.80 (C2 dimethoxybenzamide), 112.86 (C3 furan), 114.80 (C4 furan), 118.22 (C olefinic), 120.86 (C4 bromophenyl), 121.93 (C6 dimethoxybenzamide), 126.43 (C olefinic), 126.95 (C1 dimethoxybenzamide), 128.04 (C2,6 bromophenyl), 131.93 (C3,5 bromophenyl), 134.40 (C1 bromophenyl), 145.22 (C5 furan), 148.66 (C2 furan), 149.74 (C4 thiazole), 149.97 (C3 dimethoxybenzamide), 152.16 (C4 dimethoxybenzamide), 165.37 (C=O hydrazide), 165.76 (C=O dimethoxybenzamide), 173.20 (C2 thiazole). Anal. Calcd. for $C_{25}H_{21}ClN_4O_5S$ (524.98): C, 57.20; H, 4.03; N, 10.67. Found: C, 57.33; H, 3.95; N, 10.76.

(Z)-*N*-(1-(Furan-2-yl)-3-(2-(4-(3-nitrophenyl)thiazol-2-yl)hydrazinyl)-3-oxoprop-1-en-2-yl)-3,4-dimethoxybenzamide (**3c**)

Pale yellow powder (318 mg, 59%), m.p. 222–224 °C. ^{1}H-NMR (400 MHz, DMSO-d_6, δ ppm): 3.85 (s, 6H, 2OCH_3), 6.62 (dd, *J* = 3.3, 1.8 Hz, 1H, furan CH), 6.79 (d, *J* = 3.4 Hz, 1H, furan CH), 7.10 (d, *J* = 8.5 Hz, 1H, arom.CH), 7.15 (s, 1H, olefinic CH), 7.59 (s, 1H, thiazole CH), 7.66 (s, 1H, arom.CH), 7.70 (t, *J* = 8.0 Hz, 2H, arom.CH), 7.80–7.83 (m, 1H, arom.CH), 8.14 (dd, *J* = 8.1, 1.7 Hz, 1H, furan CH), 8.29 (d, *J* = 7.8 Hz, 1H, arom.CH), 8.65 (s, 1H, arom.CH), 9.72 (s, 1H, NH), 9.81 (s, 1H, NH), 10.61 (s, 1H, NH). ^{13}C-NMR (100 MHz, DMSO-d_6, δ ppm): 56.10 (OCH_3), 56.14 (OCH_3), 106.36 (C5 thiazole), 111.37 (C5 dimethoxybenzamide), 111.80 (C2 dimethoxybenzamide), 112.86 (C3 furan), 114.85 (C4 furan), 118.21 (C olefinic), 120.39 (C5 nitrophenyl), 121.94 (C6 dimethoxybenzamide), 122.42 (C4 nitrophenyl), 126.42 (C olefinic), 126.91 (C1 dimethoxybenzamide), 130.66 (C2 nitrophenyl), 132.08 (C6 nitrophenyl), 136.71 (C1 nitrophenyl), 145.25 (C5 furan), 148.53 (C3 nitrophenyl), 148.66 (C2 furan), 148.76 (C4 thiazole), 149.97 (C3 dimethoxybenzamide), 152.17 (C4 dimethoxybenzamide), 165.41 (C=O hydrazide), 165.78 (C=O dimethoxybenzamide), 173.56 (C2 thiazole). Anal. Calcd. for $C_{25}H_{21}N_5O_7S$ (535.53): C, 56.07; H, 3.95; N, 13.08. Found: C, 55.88; H, 4.03; N, 13.19.

(Z)-*N*-(1-(Furan-2-yl)-3-oxo-3-(2-(4-phenylthiazol-2-yl)hydrazinyl)prop-1-en-2-yl)-3,4,5-trimethoxybenzamide (**4a**)

Buff powder (283 mg, 65%), m.p. 197–199 °C. ^{1}H-NMR (400 MHz, DMSO-d_6, δ ppm): 3.75 (s, 3H, OCH_3), 3.88 (s, 6H, 2OCH_3), 6.63 (s, 1H, furan CH), 6.80 (d, *J* = 2.8 Hz, 1H, furan CH), 7.18 (s, 1H, olefinic CH), 7.25 (s, 1H, thiazole CH), 7.29 (t, *J* = 7.3 Hz, 1H, arom.CH), 7.38 (d, *J* = 7.8 Hz, 2H, arom.CH), 7.41 (s, 2H, arom.CH), 7.83 (s, 2H, arom.CH), 7.85 (s, 1H, furan CH), 9.56 (s, 1H, NH), 9.88 (s, 1H, NH), 10.57 (s, 1H, NH). ^{13}C-NMR (100 MHz, DMSO-d_6, δ ppm): 56.55 (2OCH_3), 60.59 (OCH_3), 103.63 (C5 thiazole), 106.08 (C2,6 trimethoxybenzamide), 112.90 (C3 furan), 115.12 (C4 furan), 118.46 (C olefinic), 126.01 (C2,6 phenyl), 126.62 (C olefinic), 127.90 (C4 phenyl), 129.01 (C3,5 phenyl), 129.31 (C1 trimethoxybenzamide), 135.19, (C1 phenyl) 140.83 (C4 trimethoxybenzamide), 145.39 (C5 furan), 149.88 (C2 furan), 150.96 (C4 thiazole), 153.02 (C3,5 trimethoxybenzamide), 165.27 (C=O hydrazide), 165.75 (C=O trimethoxybenzamide), 173.03 (C2 thiazole). Anal. Calcd. for $C_{24}H_{24}N_2O_6$ (436.46): C, 66.04; H, 5.54; N, 6.42. Found: C, 65.88; H, 5.68; N, 6.33.

(Z)-*N*-(3-(2-(4-(4-Chlorophenyl)thiazol-2-yl)hydrazinyl)-1-(furan-2-yl)-3-oxoprop-1-en-2-yl)-3,4,5-trimethoxybenzamide (**4b**)

Yellow powder (383 mg, 69%), m.p. 218–220 °C. ^{1}H-NMR (400 MHz, DMSO-d_6, δ ppm): 3.75 (s, 3H, OCH_3), 3.87 (s, 6H, 2OCH_3), 6.63 (dd, *J* = 3.4, 1.8 Hz, 1H, furan CH), 6.81 (d, *J* = 3.4 Hz, 1H, furan CH), 7.18 (s, 1H, olefinic CH), 7.32 (s, 1H, thiazole CH), 7.41 (s, 2H, arom.CH), 7.45 (d, *J* = 8.6 Hz, 2H, arom.CH), 7.83 (d, *J* = 1.4 Hz, 1H, furan CH), 7.86 (d, *J* = 8.6 Hz, 2H, arom.CH), 9.61 (s, 1H, NH), 9.88 (s, 1H, NH), 10.56 (s, 1H, NH). ^{13}C-NMR (100 MHz, DMSO-d_6, δ ppm): 56.55 (2OCH_3), 60.58 (OCH_3), 104.42 (C5 thiazole), 106.10 (C2,6 trimethoxybenzamide), 112.90 (C3 furan), 115.13 (C4 furan), 118.45 (C olefinic), 126.63 (C olefinic), 127.72 (C2,6 chlorophenyl), 129.02 (C3,5 chlorophenyl), 129.31 (C1 trimethoxybenzamide), 132.27 (C1 chlorophenyl), 134.05 (C4 chlorophenyl), 140.84 (C4 trimethoxybenzamide), 145.39 (C5 furan), 149.70 (C2 furan), 149.88 (C4 thiazole), 153.02 (C3,5 trimethoxybenzamide), 165.25 (C=O hydrazide), 165.71 (C=O trimethoxybenzamide), 173.17 (C2 thiazole). Anal. Calcd. for $C_{26}H_{23}ClN_4O_6S$ (555.00): C, 56.27; H, 4.18; N, 10.09. Found: C, 56.39; H, 4.23; N, 9.93.

(Z)-*N*-(3-(2-(4-(4-Bromophenyl)thiazol-2-yl)hydrazinyl)-1-(furan-2-yl)-3-oxoprop-1-en-2-yl)-3,4,5-trimethoxybenzamide (**4c**)

Pale yellow powder (413 mg, 69%), m.p. 216–218 °C. ^{1}H-NMR (400 MHz, DMSO-d_6, δ ppm): 3.75 (s, 3H, OCH_3), 3.87 (s, 6H, 2OCH_3), 6.62 (dd, *J* = 3.4, 1.8 Hz, 1H, furan CH), 6.80 (d, *J* = 3.0 Hz, 1H, furan CH), 7.17 (s, 1H, olefinic CH), 7.33 (s, 1H, thiazole CH), 7.41 (s, 2H, arom.CH), 7.58 (d, *J* = 8.6 Hz, 2H, arom.CH), 7.77–7.81 (m, 2H, arom.CH), 7.83 (d, *J* = 1.3 Hz, 1H, furan CH), 9.61 (s, 1H, NH), 9.88 (s, 1H, NH), 10.57 (s, 1H, NH). ^{13}C-NMR (100 MHz, DMSO-d_6, δ ppm): 56.55 (2OCH_3), 60.58 (OCH_3), 104.50 (C5 thiazole), 106.09 (C2,6 trimethoxybenzamide), 112.89 (C3 furan), 115.12 (C4 furan), 118.54 (C olefinic), 120.86 (C4 bromophenyl), 126.64 (C olefinic), 128.03 (C2,6 bromophenyl), 129.31 (C1 trimethoxybenzamide), 131.93 (C3,5 bromophenyl), 134.40 (C1 bromophenyl), 140.84 (C4 trimethoxybenzamide), 145.38 (C5 furan), 149.74 (C2 furan), 149.89 (C4 thiazole), 153.02 (C3,5 trimethoxybenzamide), 165.28 (C=O hydrazide), 165.70 (C=O trimethoxybenzamide), 173.16 (C2 thiazole). Anal. Calcd. for $C_{26}H_{23}BrN_4O_6S$ (599.45): C, 52.09; H, 3.87; N, 9.35. Found: C, 51.97; H, 3.96; N, 9.43.

(Z)-*N*-(1-(Furan-2-yl)-3-(2-(4-(3-nitrophenyl)thiazol-2-yl)hydrazinyl)-3-oxoprop-1-en-2-yl)-3,4,5-trimethoxybenzamide (**4d**)

Buff powder (374 mg, 66%), m.p. 214–216 °C. ^{1}H-NMR (400 MHz, DMSO-d_6, δ ppm): 3.75 (s, 3H, OCH_3), 3.88 (s, 6H, 2OCH_3), 6.63 (dd, *J* = 3.3, 1.8 Hz, 1H, furan CH), 6.81 (d, *J* = 3.3 Hz, 1H, furan CH), 7.18 (s, 1H, olefinic CH), 7.41 (s, 2H, arom.CH), 7.59 (s, 1H, thiazole CH), 7.70 (t, *J* = 8.0 Hz, 1H, arom.CH), 7.80–7.88 (m, 1H, arom.CH), 8.10–8.20 (m, 1H, arom.CH), 8.29 (d, *J* = 7.9 Hz, 1H, furan CH), 8.66 (s, 1H, arom.CH), 9.73 (s, 1H, NH), 9.90 (s, 1H, NH), 10.62 (s, 1H, NH). ^{13}C-NMR (100 MHz, DMSO-d_6, δ ppm): 56.55 (2OCH_3), 60.59 (OCH_3), 106.10 (C2,6 trimethoxybenzamide), 106.37 (C5 thiazole), 112.90 (C3 furan), 115.17 (C4 furan), 118.43 (C olefinic), 120.43 (C5 nitrophenyl), 122.43 (C4 nitrophenyl), 126.59 (C olefinic), 129.30 (C1 trimethoxybenzamide), 130.66 (C2 nitrophenyl), 132.07 (C6 nitrophenyl), 136.70 (C1 nitrophenyl), 140.85 (C4 trimethoxybenzamide), 145.42 (C5 furan), 148.52 (C3 nitrophenyl), 148.75 (C2 furan), 149.88 (C4 thiazole), 153.02 (C3,5 trimethoxybenzamide), 165.27 (C=O hydrazide), 165.79 (C=O trimethoxybenzamide), 173.51 (C2 thiazole). Anal. Calcd. for $C_{26}H_{23}N_5O_8S$ (565.55): C, 55.22; H, 4.10; N, 12.38. Found: C, 55.11; H, 4.19; N, 12.31.

(Z)-*N*-(1-(Furan-2-yl)-3-(2-(4-(3-methoxyphenyl)thiazol-2-yl)hydrazinyl)-3-oxoprop-1-en-2-yl)-3,4,5-trimethoxybenzamide (**4e**)

Yellow powder (333 mg, 61%), m.p. 231–233 °C. ^{1}H-NMR (400 MHz, DMSO-d_6, δ ppm): 3.75 (s, 3H, OCH_3), 3.80 (s, 3H, OCH_3), 3.88 (s, 6H, 2OCH_3), 6.60–6.66 (m, 1H, furan CH), 6.80 (d, *J* = 3.1 Hz, 1H, furan CH), 6.86 (dd, *J* = 8.2, 2.2 Hz, 1H, arom.CH), 7.18 (s, 1H,

olefinic CH), 7.28 (s, 1H, thiazole CH), 7.31 (d, *J* = 7.9 Hz, 1H, arom.CH), 7.42 (d, *J* = 9.7 Hz, 4H, arom.CH), 7.83 (s, 1H, furan CH), 9.57 (s, 1H, NH), 9.87 (s, 1H, NH), 10.57 (s, 1H, NH). ^{13}C-NMR (100 MHz, DMSO-d_6, δ ppm): 55.52 (OCH_3), 56.55 ($2OCH_3$), 60.59 (OCH_3), 104.03 (C5 thiazole), 106.04 (C2,6 trimethoxybenzamide), 111.37 (C2 methoxyphenyl), 112.90 (C3 furan), 113.63 (C4 methoxyphenyl), 115.10 (C4 furan), 118.42 (C olefinic), 118.46 (C6 methoxyphenyl), 126.64 (C olefinic), 129.32 (C1 trimethoxybenzamide), 130.05 (C5 methoxyphenyl), 136.59 (C1 methoxyphenyl), 140.83 (C4 trimethoxybenzamide), 145.37 (C5 furan), 149.89 (C2 furan), 150.79 (C4 thiazole), 152.99 (C3,5 trimethoxybenzamide), 159.94 (C3 methoxyphenyl), 165.28 (C=O hydrazide), 165.71 (C=O trimethoxybenzamide), 172.90 (C2 thiazole). Anal. Calcd. for $C_{27}H_{26}N_4O_7S$ (550.58): C, 58.90; H, 4.76; N, 10.18. Found: C, 59.04; H, 4.88; N, 10.07.

4.1.4. General Procedure for the Synthesis of (E)-Ethyl 2-(2-(2-((Z)-2-(arylamido)-3-(furan-2-yl)acryloyl)hydrazinyl)thiazol-4(5H)-ylidene)acetates **5a,b**

A mixture of appropriate hydrazinecarbothioamide **2a,b** (10 mmol), ethyl 4-chloroaceto acetate (1.35 mL, 10 mmol) and potassium carbonate anhydrous (164 mg, 12 mmol) was stirred in dry DMF (20 mL) for 12 h. After completion of the reaction as monitored by a TLC analysis, the solution was poured onto crushed ice, filtered off, dried and crystallized from DMF/ethanol (1:1) to furnish the title compound **5a,b**.

(E)-Ethyl 2-(2-(2-((Z)-2-(3,4-dimethoxybenzamido)-3-(furan-2-yl)acryloyl)hydrazinyl)thiazol-4(5H)-ylidene)acetate (**5a**)

Yellow powder (267 mg, 53%), m.p. 211–213 °C. ^{1}H-NMR (400 MHz, DMSO-d_6, δ ppm): 1.20 (t, *J* = 7.1 Hz, 3H, CH_3), 3.54 (s, 2H, CH_2 thiazole), 3.85 (s, 6H, $2OCH_3$), 4.08 (q, *J* = 7.1 Hz, 2H, CH_2), 6.57 (s, 1H, olefinic CH), 6.59–6.62 (m, 1H, furan CH), 6.76 (d, *J* = 3.3 Hz, 1H, furan CH), 7.09 (d, *J* = 8.5 Hz, 1H, arom.CH), 7.11–7.15 (m, 1H, olefinic CH), 7.64 (s, 1H, arom.CH), 7.69 (d, *J* = 8.4 Hz, 1H, arom.CH), 7.79 (s, 1H, furan CH), 9.40 (s, 1H, NH), 9.79 (d, *J* = 5.9 Hz, 1H, NH), 10.50 (d, *J* = 5.9 Hz, 1H, NH). ^{13}C-NMR (100 MHz, DMSO-d_6, δ ppm): 14.56 ($OCH_2\underline{CH_3}$), 37.51 (C5 thiazole), 55.38 (OCH_3), 56.14 (OCH_3), 60.70 ($O\underline{CH_2}CH_3$), 105.54 (C olefinic), 111.35 (C5 dimethoxybenzamide), 111.80 (C2 dimethoxybenzamide), 112.84 (C3 furan), 114.72 (C4 furan), 118.22 (C olefinic), 121.93 (C6 dimethoxybenzamide), 126.43 (C1 dimethoxybenzamide), 126.93 (C olefinic), 145.15 (C5 furan), 145.54 (C2 furan), 148.64 (C2 thiazole), 149.96 (C3 dimethoxybenzamide), 152.14 (C4 dimethoxybenzamide), 165.30 (C4 thiazole), 165.73 (C=O hydrazide), 170.51 (C=O dimethoxybenzamide), 173.06 (C=O ester). Anal. Calcd. for $C_{23}H_{24}N_4O_7S$ (500.52): C, 55.19; H, 4.83; N, 11.19. Found: C, 55.10; H, 4.91; N, 11.34.

(E)-Ethyl 2-(2-(2-((Z)-3-(furan-2-yl)-2-(3,4,5-trimethoxybenzamido)acryloyl)hydrazinyl)thiazol-4(5H)-ylidene)acetate (**5b**)

White powder (371 mg, 70%), m.p. 216–218 °C. ^{1}H-NMR (400 MHz, DMSO-d_6, δ ppm): 1.19 (t, *J* = 7.1 Hz, 3H, CH_3), 3.54 (s, 2H, CH_2 thiazole), 3.75 (s, 3H, OCH_3), 3.87 (s, 6H, $2OCH_3$), 4.08 (q, *J* = 7.1 Hz, 2H, CH_2), 6.57 (s, 1H, olefinic CH), 6.62 (dd, *J* = 3.4, 1.8 Hz, 1H, furan CH), 6.79 (d, *J* = 3.4 Hz, 1H, furan CH), 7.14 (s, 1H, olefinic CH), 7.39 (s, 2H, arom.CH), 7.82 (d, *J* = 1.4 Hz, 1H, furan CH), 9.41 (s, 1H, NH), 9.86 (s, 1H, NH), 10.48 (s, 1H, NH). ^{13}C-NMR (100 MHz, DMSO-d_6, δ ppm): 14.57 ($OCH_2\underline{CH_3}$), 37.52 (C5 thiazole), 56.54 ($2OCH_3$), 60.58 (OCH_3), 60.69 ($O\underline{CH_2}CH_3$), 105.56 (C olefinic), 106.07 (C2,6 trimethoxybenzamide), 112.88 (C3 furan), 115.03 (C4 furan), 118.38 (C olefinic), 126.66 (C olefinic), 129.31 (C1 trimethoxybenzamide), 140.82 (C4 trimethoxybenzamide), 145.34 (C5 furan), 145.59 (C2 furan), 149.88 (C2 thiazole), 153.01 (C3,5 trimethoxybenzamide), 165.15 (C4 thiazole), 165.66 (C=O hydrazide), 170.50 (C=O trimethoxybenzamide), 173.03 (C=O ester). Anal. Calcd. for $C_{24}H_{26}N_4O_8S$ (530.55): C, 54.33; H, 4.94; N, 10.56. Found: C, 54.42; H, 5.02; N, 10.44.

4.2. Biological Study

4.2.1. MTT Cytotoxicity Assay

An MTT colorimetric assay was carried out to investigate the impact of the newly synthesized thiazolyl derivatives **3a-5b** on a breast carcinoma (MDA-MB-231) cell line. See Section S4.2.1 in Supplementary Materials.

4.2.2. VEGFR-2 Inhibition Assay

A VEGFR-2 inhibition assay was performed for thiazolyl derivatives **4b, 4d** and **4d** compared with sorafenib according to a previously reported method [37]. See Section S4.2.2 in Supplementary Materials.

4.2.3. Cell Cycle Analysis

A cell cycle analysis in MDA-MB-231 cells was carried out by a FACS analysis according to the manufacturer's directions. See Section S4.2.3 in Supplementary Materials.

4.2.4. Annexin V/FITC Staining Assay

An annexin V/FITC double staining analysis in MDA-MB-231 cells was carried out by a FACS analysis according to the manufacturer's directions. See Section S4.2.4 in Supplementary Materials.

4.2.5. Mitochondrial Membrane Potential

The MMP was measured by a flow cytometry analysis in MDA-MB-231 cells according to the manufacturer's directions. See Section S4.2.5 in Supplementary Materials.

4.2.6. Effect on p53, Bax and Bcl-2

Apoptotic marker p53 was measured in MDA-MB-231 cells using an ELISA according to the manufacturer's directions. See Section S4.2.6 in Supplementary Materials.

4.2.7. Molecular Docking Study

The docking study was carried out using molecular operating environment (MOE 2015.10). See Section S4.2.7 in Supplementary Materials.

Supplementary Materials: The following supporting information can be downloaded at: https://www.mdpi.com/article/10.3390/sym14091814/s1, Figure S1: ^{1}H-NMR spectrum of compound **2a**, Figure S2: ^{13}C-NMR spectrum of compound **2a**, Figure S3: ^{1}H-NMR spectrum of compound **2b**, Figure S4: ^{1}H-NMR spectrum of compound **3a**, Figure S5: ^{13}C-NMR spectrum of compound **3a,** Figure S6: ^{1}H-NMR spectrum of compound **3b**, Figure S7: ^{13}C-NMR spectrum of compound **3b**, Figure S8: ^{1}H-NMR spectrum of compound **3c**, Figure S9: ^{13}C-NMR spectrum of compound **3c**, Figure S10: ^{1}H-NMR spectrum of compound **4a**, Figure S11: ^{13}C-NMR spectrum of compound **4a**, Figure S12: ^{1}H-NMR spectrum of compound **4b**, Figure S13: ^{13}C-NMR spectrum of compound **4b,** Figure S14: ^{1}H-NMR spectrum of compound **4c,** Figure S15: ^{13}C-NMR spectrum of compound **4c**, Figure S16: ^{1}H-NMR spectrum of compound **4d**, Figure S17: ^{13}C-NMR spectrum of compound **4d,** Figure S18: ^{1}H-NMR spectrum of compound **4e**, Figure S19: ^{13}C-NMR spectrum of compound **4e**, Figure S20: ^{1}H-NMR spectrum of compound **5a**, Figure S21: ^{13}C-NMR spectrum of compound **5a**, Figure S22: ^{1}H-NMR spectrum of compound **5b**, Figure S23: ^{13}C-NMR spectrum of compound **5b**.

Author Contributions: Conceptualization, I.Z., E.F., M.A., N.M.A. and T.A.-W.; methodology, O.A.A.A., F.G.E., A.A.S., S.A. and K.O.M.; data curation, T.A.-W., E.F., S.A., A.H.A.A., W.M.A., O.A.A.A. and I.Z.; software, F.G.E., K.O.M., W.M.A. and I.Z.; resources, T.A.-W., N.M.A., F.G.E., A.A.S., S.A. and I.Z.; supervision, K.O.M. and I.Z.; funding acquisition, T.A.-W., M.A., E.F., F.G.E., O.A.A.A. and S.A.; original draft preparation, I.Z. and T.A.-W.; Writing, review, and editing, all authors. All authors have read and agreed to the published version of the manuscript.

Funding: The authors extend their appreciation to the Princess Nourah bint Abdulrahman University Researchers Supporting Project number (PNURSP2022R25), Princess Nourah bint Abdulrahman

University, Riyadh, Saudi Arabia & Deanship of Scientific Research, King Khalid University, KSA (research group project number (RGP. 2/113/43).

Institutional Review Board Statement: Not applicable.

Informed Consent Statement: Not applicable.

Data Availability Statement: All data are available within the manuscript.

Acknowledgments: The authors extend their appreciation to the Princess Nourah bint Abdulrahman University Researchers Supporting Project number (PNURSP2022R25), Princess Nourah bint Abdulrahman University, Riyadh, Saudi Arabia & Deanship of Scientific Research, King Khalid University, KSA (research group project number (RGP. 2/113/43). The authors are grateful to Taif University for carrying out the cytotoxicity testing. The authors thank all members of the department of biology, College of Science, University of Jeddah, Jeddah, Saudi Arabia for carrying out VEGFR-2 inhibition assay.

Conflicts of Interest: The authors declare no conflict of interest.

References

1. Al-Joufi, F.; Setia, A.; Salem-Bekhit, M.; Sahu, R.; Alqahtani, F.; Widyowati, R.; Aleanizy, F. Molecular Pathogenesis of Colorectal Cancer with an Emphasis on Recent Advances in Biomarkers, as Well as Nanotechnology-Based Diagnostic and Therapeutic Approaches. *Nanomaterials* **2022**, *12*, 169. [CrossRef] [PubMed]
2. McNevin, C.S.; Cadoo, K.; Baird, A.-M.; Murchan, P.; Sheils, O.; McDermott, R.; Finn, S. Pathogenic BRCA Variants as Biomarkers for Risk in Prostate Cancer. *Cancers* **2021**, *13*, 5697. [CrossRef] [PubMed]
3. Bradley, R.; Braybrooke, J.; Gray, R.; Hills, R.K.; Liu, Z.; Pan, H.; Peto, R.; Dodwell, D.; McGale, P.; Taylor, C.; et al. Aromatase inhibitors versus tamoxifen in premenopausal women with oestrogen receptor-positive early-stage breast cancer treated with ovarian suppression: A patient-level meta-analysis of 7030 women from four randomised trials. *Lancet Oncol.* **2022**, *23*, 382–392. [CrossRef]
4. Klement, G.; Huang, P.; Mayer, B.; Green, S.K.; Man, S.; Bohlen, P.; Hicklin, D.; Kerbel, R.S. Differences in Therapeutic Indexes of Combination Metronomic Chemotherapy and an Anti-VEGFR-2 Antibody in Multidrug-resistant Human Breast Cancer Xenografts1. *Clin. Cancer Res.* **2002**, *8*, 221–232. [PubMed]
5. Shaikh, S.S.; Emens, L.A. Current and emerging biologic therapies for triple negative breast cancer. *Expert Opin. Biol. Ther.* **2022**, *22*, 591–602. [CrossRef]
6. Abdalla, Y.O.A.; Subramaniam, B.; Nyamathulla, S.; Shamsuddin, N.; Arshad, N.M.; Mun, K.S.; Awang, K.; Nagoor, N.H. Natural Products for Cancer Therapy: A Review of Their Mechanism of Actions and Toxicity in the Past Decade. *J. Trop. Med.* **2022**, *2022*, e5794350. [CrossRef]
7. Najmi, A.; Javed, S.A.; Al Bratty, M.; Alhazmi, H.A. Modern Approaches in the Discovery and Development of Plant-Based Natural Products and Their Analogues as Potential Therapeutic Agents. *Molecules* **2022**, *27*, 349. [CrossRef]
8. Formica, M.L.; Alfonso, H.G.A.; Palma, S.D. Biological drug therapy for ocular angiogenesis: Anti-VEGF agents and novel strategies based on nanotechnology. *Pharmacol. Res. Perspect.* **2021**, *9*, e00723. [CrossRef]
9. Das, R.; Choithramani, A.; Shard, A. A molecular perspective for the use of type IV tyrosine kinase inhibitors as anticancer therapeutics. *Drug Discov. Today* **2022**, *27*, 808–821. [CrossRef]
10. Cordover, E.; Minden, A.; Lehman, S.; Zhao, O. Signaling pathways downstream to receptor tyrosine kinases: Targets for cancer treatment. *J. Cancer Metastasis Treat.* **2020**, *2020*, 1–19. [CrossRef]
11. Behl, T.; Rana, T.; Alotaibi, G.H.; Shamsuzzaman, M.; Naqvi, M.; Sehgal, A.; Singh, S.; Sharma, N.; Almoshari, Y.; Abdellatif, A.A.H.; et al. Polyphenols inhibiting MAPK signalling pathway mediated oxidative stress and inflammation in depression. *Biomed. Pharmacother.* **2022**, *146*, 112545–112558. [CrossRef] [PubMed]
12. Saraon, P.; Pathmanathan, S.; Snider, J.; Lyakisheva, A.; Wong, V.; Stagljar, I. Receptor tyrosine kinases and cancer: Oncogenic mechanisms and therapeutic approaches. *Oncogene* **2021**, *40*, 4079–4093. [CrossRef] [PubMed]
13. Cheng, K.; Liu, C.-F.; Rao, G.-W. Anti-angiogenic Agents: A Review on Vascular Endothelial Growth Factor Receptor-2 (VEGFR-2) Inhibitors. *Curr. Med. Chem.* **2021**, *28*, 2540–2564. [CrossRef]
14. Osude, C.; Lin, L.; Patel, M.; Eckburg, A.; Berei, J.; Kuckovic, A.; Dube, N.; Rastogi, A.; Gautam, S.; Smith, T.J.; et al. Mediating EGFR-TKI Resistance by VEGF/VEGFR Autocrine Pathway in Non-Small Cell Lung Cancer. *Cells* **2022**, *11*, 1694. [CrossRef]
15. Toaldo, M.B.; Salvatore, V.; Marinelli, S.; Palamà, C.; Milazzo, M.; Croci, L.; Venerandi, L.; Cipone, M.; Bolondi, L.; Piscaglia, F. Use of VEGFR-2 Targeted Ultrasound Contrast Agent for the Early Evaluation of Response to Sorafenib in a Mouse Model of Hepatocellular Carcinoma. *Mol. Imaging Biol.* **2015**, *17*, 29–37. [CrossRef] [PubMed]
16. AbdElhameid, M.K.; Labib, M.B.; Negmeldin, A.T.; Al-Shorbagy, M.; Mohammed, M.R. Design, synthesis, and screening of ortho-amino thiophene carboxamide derivatives on hepatocellular carcinomaas VEGFR-2Inhibitors. *J. Enzym. Inhib. Med. Chem.* **2018**, *33*, 1472–1493. [CrossRef] [PubMed]

17. El-Adl, K.; El-Helby, A.-G.A.; Sakr, H.; Ayyad, R.R.; Mahdy, H.A.; Nasser, M.; Abulkhair, H.S.; El-Hddad, S.S.A. Design, synthesis, molecular docking, anticancer evaluations, and in silico pharmacokinetic studies of novel 5-[(4-chloro/2,4-dichloro)benzylidene]thiazolidine-2,4-dione derivatives as VEGFR-2 inhibitors. *Arch. Pharm.* **2021**, *354*, e2000279. [CrossRef]
18. Kassab, A.E.; El-Dash, Y.; Gedawy, E.M. Novel pyrazolopyrimidine urea derivatives: Synthesis, antiproliferative activity, VEGFR-2 inhibition, and effects on the cell cycle profile. *Arch. Pharm.* **2020**, *353*, e1900319. [CrossRef]
19. AbdelHaleem, A.; Mansour, A.O.; AbdelKader, M.; Arafa, R.K. Selective VEGFR-2 inhibitors: Synthesis of pyridine derivatives, cytotoxicity and apoptosis induction profiling. *Bioorg. Chem.* **2020**, *103*, 104222–104237. [CrossRef]
20. Marzouk, A.A.; Abdel-Aziz, S.A.; Abdelrahman, K.S.; Wanas, A.S.; Gouda, A.M.; Youssif, B.G.M.; Abdel-Aziz, M. Design and synthesis of new 1,6-dihydropyrimidin-2-thio derivatives targeting VEGFR-2: Molecular docking and antiproliferative evaluation. *Bioorg. Chem.* **2020**, *102*, 104090–104099. [CrossRef] [PubMed]
21. Dawood, D.H.; Nossier, E.S.; Ali, M.M.; Mahmoud, A.E. Synthesis and molecular docking study of new pyrazole derivatives as potent anti-breast cancer agents targeting VEGFR-2 kinase. *Bioorg. Chem.* **2020**, *101*, 103916–103928. [CrossRef]
22. Tian, Y.; Lei, Y.; Fu, Y.; Sun, H.; Wang, J.; Xia, F. Molecular mechanisms of resistance to tyrosine kinase inhibitors associated with hepatocellular carcinoma. *Curr. Cancer Drug Targets* **2022**, *22*, 454–462. [CrossRef] [PubMed]
23. Abdallah, A.E.; Mabrouk, R.R.; Elnagar, M.R.; Farrag, A.M.; Kalaba, M.H.; Sharaf, M.H.; El-Fakharany, E.M.; Bakhotmah, D.A.; Elkaeed, E.B.; Al Ward, M.M.S. New Series of VEGFR-2 Inhibitors and Apoptosis Enhancers: Design, Synthesis and Biological Evaluation. *Drug Des. Dev. Ther.* **2022**, *16*, 587–606. [CrossRef] [PubMed]
24. Arshad, M.F.; Alam, A.; Alshammari, A.A.; Alhazza, M.B.; Alzimam, I.M.; Alam, M.A.; Mustafa, G.; Ansari, M.S.; Alotaibi, A.M.; Alotaibi, A.A.; et al. Thiazole: A Versatile Standalone Moiety Contributing to the Development of Various Drugs and Biologically Active Agents. *Molecules* **2022**, *27*, 3994. [CrossRef] [PubMed]
25. Raveesha, R.; Anusuya, A.M.; Raghu, A.V.; Kumar, K.Y.; Kumar, M.G.D.; Prasad, S.B.B.; Prashanth, M.K. Synthesis and characterization of novel thiazole derivatives as potential anticancer agents: Molecular docking and DFT studies. *Comput. Toxicol.* **2022**, *21*, 100202–100219. [CrossRef]
26. Litim, B.; Djahoudi, A.; Meliani, S.; Boukhari, A. Synthesis and potential antimicrobial activity of novel α-aminophosphonates derivatives bearing substituted quinoline or quinolone and thiazole moieties. *Med. Chem. Res.* **2022**, *31*, 60–74. [CrossRef]
27. Abdel-Aziz, S.A.; Taher, E.S.; Lan, P.; El-Koussi, N.A.; Salem, O.I.A.; Gomaa, H.A.M.; Youssif, B.G.M. New pyrimidine/thiazole hybrids endowed with analgesic, anti-inflammatory, and lower cardiotoxic activities: Design, synthesis, and COX-2/sEH dual inhibition. *Arch. Pharm.* **2022**, *355*, e2200024. [CrossRef]
28. Altıntop, M.D.; Sever, B.; Çiftçi, G.A.; Özdemir, A. Design, Synthesis, and Evaluation of a New Series of Thiazole-Based Anticancer Agents as Potent Akt Inhibitors. *Molecules* **2018**, *23*, 1318. [CrossRef]
29. Hassan, A.; Badr, M.; Hassan, H.A.; Abdelhamid, D.; Abuo-Rahma, G.E.D.A. Novel 4-(piperazin-1-yl)quinolin-2(1H)-one bearing thiazoles with antiproliferative activity through VEGFR-2-TK inhibition. *Bioorg. Med. Chem.* **2021**, *40*, 116168–116181. [CrossRef]
30. El-Naggar, A.M.; Zidan, A.; Elkaeed, E.B.; Taghour, M.S.; Badawi, W.A. Design, synthesis and docking studies of new hydrazinyl-thiazole derivatives as anticancer and antimicrobial agents. *J. Saudi Chem. Soc.* **2022**, *26*, 101488–101502. [CrossRef]
31. Pandrangi, S.L.; Chittineedi, P.; Chalumuri, S.S.; Meena, A.S.; Mosquera, J.A.N.; Llaguno, S.N.S.; Pamuru, R.R.; Mohiddin, G.J.; Mohammad, A. Role of Intracellular Iron in Switching Apoptosis to Ferroptosis to Target Therapy-Resistant Cancer Stem Cells. *Molecules* **2022**, *27*, 3011. [CrossRef] [PubMed]
32. Lopez, J.; Tait, S.W.G. Mitochondrial apoptosis: Killing cancer using the enemy within. *Br. J. Cancer* **2015**, *112*, 957–962. [CrossRef] [PubMed]
33. Ran, F.; Li, W.; Qin, Y.; Yu, T.; Liu, Z.; Zhou, M.; Liu, C.; Qiao, T.; Li, X.; Yousef, R.G.; et al. Inhibition of Vascular Smooth Muscle and Cancer Cell Proliferation by New VEGFR Inhibitors and Their Immunomodulator Effect: Design, Synthesis, and Biological Evaluation. *Oxid. Med. Cell. Longev.* **2021**, *2021*, 8321400. [CrossRef]
34. Engeland, K. Cell cycle regulation: p53-p21-RB signaling. *Cell Death Differ.* **2022**, *29*, 946–960. [CrossRef] [PubMed]
35. Marei, H.E.; Althani, A.; Afifi, N.; Hasan, A.; Caceci, T.; Pozzoli, G.; Morrione, A.; Giordano, A.; Cenciarelli, C. p53 signaling in cancer progression and therapy. *Cancer Cell Int.* **2021**, *21*, 703–718. [CrossRef]
36. Li, A.M.; Boichard, A.; Kurzrock, R. Mutated TP53 is a marker of increased VEGF expression: Analysis of 7,525 pan-cancer tissues. *Cancer Biol. Ther.* **2020**, *21*, 95–100. [CrossRef] [PubMed]
37. Zaki, I.; Masoud, R.E.; Hamoud, M.M.S.; Ali, O.A.A.; Abualnaja, M.; Fayad, E.; Almaaty, A.H.A.; Elnaghia, L.K. Design, synthesis and cytotoxicity screening of new synthesized pyrimidine-5-carbonitrile derivatives showing marked apoptotic effect. *J. Mol. Struct.* **2022**, *1259*, 132749–132762. [CrossRef]